Biochimica et Biophysica Acta 1787 (2009) 882–889

Contents lists available at ScienceDirect

Biochimica et Biophysica Acta

journal homepage: www.elsevier.com/locate/bbabio

The S_1 split signal of photosystem II; a tyrosine–manganese coupled interaction

Nicholas Cox [a], Felix M. Ho [b], Naray Pewnim [a], Ronald Steffen [c], Paul J. Smith [a], Kajsa G.V. Havelius [b], Joseph L. Hughes [c], Lesley Debono [c], Stenbjörn Styring [b], Elmars Krausz [c], Ron J. Pace [a,*]

[a] Department of Chemistry, College of Science, Australian National University, Canberra, ACT 0200, Australia
[b] Department of Photochemistry and Molecular Science, Ångström Laboratory, Uppsala University, P.O. Box 523, SE-751 20, Uppsala, Sweden
[c] Research School of Chemistry, Australian National University, Canberra, ACT 0200, Australia

ARTICLE INFO

Article history:
Received 10 September 2008
Received in revised form 26 March 2009
Accepted 30 March 2009
Available online 9 April 2009

Keywords:
S_1 split signal
Carotenoid
Chlorophyll
Cytochrome b_{559}
Pheophytin
Tyrosine
Exchange coupled interaction

ABSTRACT

Detailed optical and EPR analyses of states induced in dark-adapted PS II membranes by cryogenic illumination permit characterization and quantification of all pigment derived donors and acceptors, as well as optically silent (in the visible, near infrared) species which are EPR active. Near complete turnover formation of $Q_{\bar{A}}$ is seen in all centers, but with variable efficiency, depending on the donor species. In minimally detergent-exposed PS II membranes, negligible (<5%) oxidation of chlorophyll or carotenoid centers occurs for illumination temperatures 5–20 K. An optically silent electron donor to $P680^+$ is observed with the same decay kinetics as the S_1 split signal. Cryogenic donors to $P680^+$ seen are: (i) transient ($t_{1/2}$ ~ 150 s) tyrosine related species, including 'split signals' (~15% total centers), (ii) reduced cytochrome b_{559} (~30–50% centers), and (iii) an organic donor, possibly an amino acid side chain, (~30% centers).

1. Introduction

Photosystem II (PS II), a pigment–protein complex found in higher plants, algae and cyanobacteria, is responsible for the catalytic conversion of water to molecular oxygen in oxygenic photosynthesis. Initial charge separation occurs upon excitation of P680 – a chlorophyll assembly bound to the D1 and D2 protein subunits – resulting in the transfer of an electron to the neighboring pheophytin ($Pheo_{D1}$) and subsequently to plastoquinone co-factors Q_A and Q_B. Electrons for the re-reduction of $P680^+$ are sourced from the oxygen evolving complex (OEC) via the redox active tyrosine residue 161 (Y_Z) of the D1 protein. The OEC, which is the water-binding site of the PS II protein, is then in turn re-reduced by electrons released upon the oxidation of water. This generates molecular oxygen and protons (for review see [1]).

Whilst the above pathway for electron donation to $P680^+$ is the most efficient one under physiological temperatures, this is not so under cryogenic illumination conditions (<20 K), where the metastable states of the OEC, so called S-states, can be trapped for spectroscopic investigations. For example, in PS II material poised in the dark stable S_1 state, secondary donor pathways normally associated with photo-protection under physiological conditions can compete with the Y_Z/OEC donation pathway in a majority of centers. This is also true for Mn-depleted and OEC inhibited samples. Possible secondary donors include cytochrome b_{559} [2,3], carotenoid [4–8] or peripheral chlorophyll (chl_Z) associated with the reaction center [9–11]. However in a fraction of centers electron donation is still thought to come from the physiological pathway discussed above. Here though the electron hole is trapped on the intervening oxidized Y_Z. This radical magnetically interacts with the OEC resolving a 'split signal' [12–20]. Nugent et al. [12] first observed a new 'split like' EPR signal induced in intact PS II samples by visible light illumination of the S_1 state at <20 K. Petrouleas et al. [19,20] demonstrated that direct excitation of the Mn cluster via near infrared illumination (NIR) at liquid helium temperatures of intact cyanobacterial PS II poised in the S_2 state generates a resonance resembling that reported by Nugent et al. [12]. The NIR-induced signal was shown to be stable (at temperatures <20 K) and had near-Curie temperature dependence (4–10 K) [19].

Very recently, Styring and co-workers [21,22] have extended the study of intermediate turnover states in functional PS II, generated by cryogenic illumination by visible and NIR light. This has identified 'split' type signals arising from PS II poised initially in the S_0, S_1 and S_3 states. Although the established protocol of direct cryogenic illumination with visible light does not generate a split signal from S_2, such a species does appear to be formed from S_3, by a NIR-induced back

Abbreviations: EPR, Electron Paramagnetic Resonance; PS II, Photosystem II; OEC, Oxygen Evolving Complex; Q_A, primary plastoquinone A acceptor of PS II; Y_Z, tyrosine Z or residue 161 of the D1 polypeptide of PS II; Y_D, tyrosine D or residue 161 of the D2 polypeptide of PS II; Pheo, pheophytin; CW, continuous wave; ZFS, zero field splitting; MA, modulation amplitude; NIR, near infrared; chl, chlorophyll; Tris, Tris(hydroxymethyl)aminomethane; PpBQ, Phenyl-p-benzoquinone

* Corresponding author. Tel.: +61 2 6125 4546; fax: +61 2 6125 8997.
E-mail address: ron.pace@anu.edu.au (R.J. Pace).

0005-2728/$ – see front matter © 2009 Elsevier B.V. All rights reserved.
doi:10.1016/j.bbabio.2009.03.023

reaction [23] analogous to that used by Koulougliotis et al. (above) for generation of an S_1 split signal from S_2. Similarly an S_2 split signal has been generated upon flash advancement in the 77–190 K range and rapid cooling to 10 K or by cryogenic illumination in methanol treated samples [23].

In this report, we have studied the S_1 split signal in higher plant PS II membrane preparations via both optical and EPR techniques. Optical measurements enabled us to quantitatively monitor $Q_{\bar{A}}$ formation as well as chlorophyll, carotenoid and cytochrome b_{559} oxidation. EPR and optical measurements made on parallel samples permitted us to quantitatively observe the development of paramagnetic species in the $g\sim2$ region as well as cytochrome oxidation. Together they allow conclusions to be drawn as to the relative donor contributions involved in cryogenic turnover of intact PS II membranes. Importantly, these measurements demonstrate that there is an 'optical silent' electron donor with the same decay kinetics of the S_1 split signal.

2. Materials and methods

2.1. PS II membrane particles

All procedures were performed between 2 and 4 °C under dim green light. The PS II membrane particles were prepared as per the procedure of Bricker et al. [24] with modifications as per Smith et al. [25] and stored in 15 mM NaCl, 10 mM $MgCl_2$, 20 mM MES (pH 6.0) (NaOH), 400 mM sucrose and 1 M glycine betaine at −88 °C until use. PS II samples used in this study experienced very short contact times with detergents during solubilization of the thylakoid membranes. Careful washing removed unbound chlorophyll without degrading the sample. The number of chlorophylls per reaction center is estimated to be 200–220 [26]. Samples were stored at ~10 mg/mL (chl) and had a typical oxygen evolving capacity of 500–800 μmol O_2/(mg chl/h).

2.2. EPR sample manipulations/experimental procedure

Unless otherwise stated, EPR and optical measurements were performed in the same glassing/cryoprotectant medium, containing 40% glycerol. Samples were washed into our PS II storage buffer (as above), diluted with 40% glycerol, and the sample concentration was adjusted to 2.5–3.5 mg chl/mL for EPR and 1 mg chl/mL for optical measurements. Similarly, formate-treated membranes were washed into the same storage buffer with added glycerol which was first flushed with argon, and 10 mM added sodium formate.

Sample loading into quartz EPR tubes was performed under dim green illumination, the samples then degassed at 4 °C using a rotary vacuum pump for 1–2 min and filled with Ar to minimize O_2 signals. This was followed by >10 min dark adaptation at ~4 °C before freezing to ~200 K (CO_2/ethanol) and subsequently to 77 K (liquid N_2). Samples were used immediately or within 24 h.

For split signal induction at cryogenic temperatures, samples were illuminated with a 125 W halogen lamp in the EPR cavity. The light beam was first passed through a water filter (path length 10 cm) and an interference filter centered at 690 nm with spectral width 10 nm, then defocused (20 mm diameter spot) directly onto the front EPR cavity grate. Recent studies in our laboratories have shown that illumination at this wavelength generates efficient P680 turnover at cryogenic temperatures [27].

EPR measurements were performed with a Bruker ESP300E spectrometer with an Oxford ESR9 liquid helium flow cryostat. A gold-chromel thermocouple directly below the sample position was used for temperature measurement. Linearity of the thermocouple reading was checked over the 5–20 K range by direct double integration of the dark stable Y_D. radical signal (also known as Signal II_{slow}) under non-saturating conditions, demonstrating the Curie behavior of the signal.

2.3. Optical sample manipulations/experimental procedure

Optical spectroscopy was performed on a custom built CCD-based spectrograph consisting of a tungsten–halogen lamp (Osram, 250 W) as a light source, a Spex 1704 0.75 m monochromator and a Princeton instruments nitrogen-cooled CCD camera (LN/CCD-1340/400-EHRB) as a detector. All lenses and windows were made of fused quartz. The sample was located in a custom built 200 μm path length cell, cooled to 5 K by means of a helium flow tube system.

Samples were loaded into the optical cells under dim green light, and then transferred to the spectrometer using a custom built light-tight lock. The lock attached directly to the He gas flow tube, eliminating stray light exposure of the sample. Samples were dark-adapted at room temperature in the lock for approximately 10 min, after which the samples were rapidly cooled to 5 K in complete darkness to ensure good glassing and low scatter.

For measurements covering the range between 500 nm and 730 nm, a 150 lines/mm grating blazed at 600 nm was used. For the range 500 nm to 1100 nm, a 50 lines/mm grating blazed at 800 nm was used. Exposure of CCD and sample was controlled by two shutters (Uniblitz VS25S2S1) synchronized with the CCD camera. Each single spectrum was acquired in a 100 ms exposure of the CCD. A single measurement induced photochemistry in less than 3% of the sample.

3. Results

3.1. Optical spectroscopy

3.1.1. Observation of $Q_{\bar{A}}$ reduction/donor oxidation by optical spectroscopy

Fig. 1A shows the optical absorption spectrum of the dark-adapted PS II membrane fragments over the 500–1000 nm region recorded at

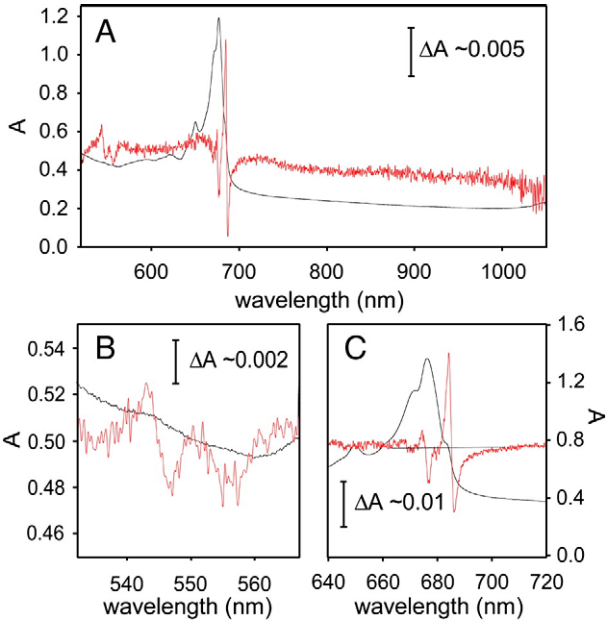

Fig. 1. Optical spectra of dark-adapted (10 min, see Materials and methods) PS II membrane particles in 40% glycerol cryoprotectant at 5 K. Black lines: absorption spectra; thin red lines: cryogenic light induced difference spectra (light-minus-dark, 5 min illumination, ~1 mW/cm^2). A: Complete Vis/NIR region where cryogenic donors/acceptors of PS II would be observed. Includes regions where chlorophyll (850 nm) and carotenoid (980 nm) radicals absorb. B: optimized spectrum of the chlorin Q_X region where the pheophytin (550 nm) and cytochrome b_{559} (557 nm) bands are readily observed. The cytochrome b_{559} band is seen as a bleach in the turnover spectrum. C: the optimized spectrum of the chlorin Q_Y region. Here Q_A− induced electrochromism of $pheo_{D1}$ is seen. Taking the zero difference base-line (thin straight line) as indicated, the turnover pattern in the 660–700 nm region is conservative, within the uncertainty of the data.

5 K. The major absorption features, between 600 and 700 nm, occur in the region of the lowest energy electronic transitions of chlorophyll and pheophytin (Q_Y transitions, Fig. 1A, C, thick solid lines). Additional bands between 560–640 nm comprise the Q_Y vibrational side structure. Two smaller features appear around 540–560 nm (Fig. 1A, B, thick solid lines). These arise from absorption by $Pheo_{D1}$ and $Pheo_{D2}$ (Q_X, second lowest transition) and reduced cytochrome b_{559}. As a consequence of the CCD detector sensitivity profile, the signal-to-noise ratio drops significantly beyond 1000 nm.

Upon cryogenic illumination (5 min green light, 1 mW/cm^2), two derivative band shift features appear in the light-minus-dark difference spectrum (red thin lines). These are centered at 684 nm and 545 nm (Fig. 1A, B, C), and have been attributed to electrochromic shifts of the Q_Y and Q_X bands of pheophytin/chlorophyll associated with the reaction center. These shifts are caused by the presence of the now negatively charge $Q_{\bar{A}}$ [28]. Therefore, the amplitudes of the shifts can be used to determine the extent of Q_A reduction, and hence sample turnover.

It can be seen in the difference spectrum of the Q_Y region (Fig. 1C) that there is also an additional shift feature centered at 674 nm. The amplitude of this shift is approximately 20–25% the dominant Q_Y shift. The origin of this shift is currently under investigation, and we presently do not assign this feature.

The only other optically observed change originating from a donor to $P680^+$ in the visible–NIR region is that from cytochrome b_{559} oxidation (Fig. 1B). In its reduced form it appears as a weak absorbance band centered around 557 nm in our samples (as confirmed by full chemical reduction of cytochrome b_{559} by dithionite; Supporting information S1). Upon illumination at 5 K this feature bleaches, giving rise to a trough in the difference spectrum (Fig. 1B, red thin line).

No spectral features above 700 nm were observed in the light-minus-dark difference spectrum, the region where absorptions by oxidized secondary donors have previously been observed (Fig. 1A). Absorbance bands at 850 nm associated with chlorophyll oxidation were not detected in the difference spectrum of any sample. Although there is a structured mix of negative and positive features in the difference spectrum in the 660–690 nm region, possibly reflecting electrochromism in coupled pigment systems, no significant net bleach was observed (Fig. 1C). This suggests negligible (<5% of reaction centers) oxidation of chlorophylls, including the chlorophyll Chl_Z [2]. In addition, no bands were observed in the 950 nm region where the carotenoid cation radicals would absorb. The large extinction coefficient (130,000–216,000 M^{-1} cm^{-1}, [4,8] and references therein) of this species allows us to exclude it as all but a trivial donor side contribution (<1% of reaction centers) in our samples.

3.1.2. Quantification of $Q_{\bar{A}}$ formation/re-oxidation and cytochrome b_{559} oxidation by optical spectroscopy

The amount of $Q_{\bar{A}}$ reduction can be estimated from the electrochromic shift feature in either Q_X or Q_Y as observed in the difference spectrum, scaled to the total absorption intensity of the Q_Y band (Fig. 1, [28]). The maximum amplitude of either shift was obtained after 5 min of illumination (1 mW/cm^2, see Materials and methods). This was taken to represent Q_A reduction in 100% of centers.

$Q_{\bar{A}}$ decay, as observed by either the Q_X or Q_Y shift features, occurs at cryogenic temperatures in all intact PS II preparations regardless of the illumination procedure (Fig. 2).[1] Approximately 15% of the $Q_{\bar{A}}$ formed decays (i.e. re-oxidized) with $t_{1/2}$~100–200 s (which is on a timescale consistent with the decay of the EPR split signal; see below). A slower decaying component is also observed with $t_{1/2}$~40–60 min in approximately ~25% of centers. The remaining $Q_{\bar{A}}$ formed does not re-oxidize within the timeframe of the experiments (>100 min).

[1] A more detailed discussion of decay rates and donor evolution will be given in a following article.

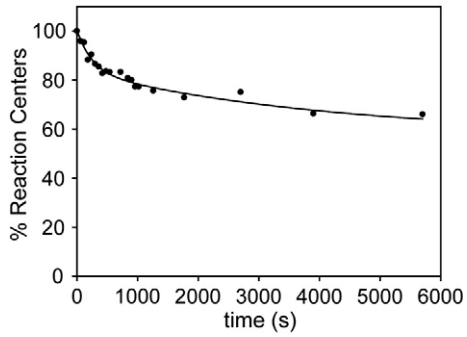

Fig. 2. Typical time course of $Q_{\bar{A}}$ decay after saturating illumination (5 min ~1 mW/cm^2, Materials and methods) at 2 K, as estimated optically from the Q_X $pheo_{D1}$ shift (Fig. 1B). Data were fitted using a double exponential function. Some sample specific variation is seen in the fitting parameters, but these are consistently within the ranges given in Table 1. The $t=0$ in the figure is when illumination was terminated.

As noted above, cytochrome b_{559} was the only donor co-factor the oxidation of which could be optically observed upon cryogenic illumination. It was also found that once oxidized, cytochrome b_{559} did not re-reduce ('rollback') during subsequent dark adaptation at 5 K. In fact, the original amount of reduced cytochrome b_{559} was not fully recovered by any annealing procedure. Therefore, this donor cannot account for any of the transiently reduced $Q_{\bar{A}}$ that decayed after illumination ceased. Given that neither chlorophyll nor carotenoid appear to be significant donors in this highly intact membrane system, and the fact that one component of the $Q_{\bar{A}}$ decay kinetics is on a timescale similar to that observed for EPR split signals, a reasonable suggestion is that at least some of the missing transient donor population is Y_Z. This would appear optically in the UV region (<300 nm). However, our present experimental arrangement does not access this region with sufficient sensitivity to reliably detect one tyrosine oxidation against the protein–pigment background.

To quantify the amount of cytochrome b_{559} that was oxidized by illumination, the amount of reduced cytochrome b_{559} originally present in the dark-adapted PS II sample was first estimated. This was done by comparing the intensity of the reduced cytochrome b_{559} absorption at 557 nm (normalized to the pheophytin (Q_X) absorption at 545 nm) in untreated PS II samples and in samples where all the cytochrome b_{559} present had been chemically reduced by dithionite treatment (Supporting information S1). It was found that cytochrome b_{559} was normally in its reduced form in more than 50% of centers in our PS II samples. After cryogenic illumination, it was found that cytochrome b_{559} oxidation was not complete, and never exceeded 50% of the PS II centers. Typically, cytochrome b_{559} was oxidized by cryogenic illumination in approximately one-third of the PS II centers in the sample.

In summary, while $Q_{\bar{A}}$ reduction and re-oxidation could be readily observed by optical spectroscopy, generally only ~30% of the donors could be assigned from readily accessible optical features (Fig. 1A). Optically observed donors and acceptors (under saturating illumination conditions) are summarized in Table 1.

3.2. EPR spectroscopy

3.2.1. $Q_{\bar{A}}$ reduction-decay as monitored by EPR spectroscopy

The extent of $Q_{\bar{A}}$ formation can also be observed in EPR through the $Q_{\bar{A}}Fe^{2+}$ EPR signal in PS II that has been treated with formate [29]. Fig. 3A shows the induction and loss of this signal upon cryogenic illumination of our dark-adapted PS II samples, as measured at the 3680 G peak (g~1.84, signal maximum; see Fig. 3B).

The formation of $Q_{\bar{A}}$ by illumination was at least bi-exponential in character (black dash lines). It was found that maximum intensity of the $Q_{\bar{A}}Fe^{2+}$ signal was achieved within ~10 min, and further illumination did not lead any significant increase.

Table 1
Optical and EPR observed donors and acceptors.

Acceptor/donor	% of RC Optical	% of RC EPR[a]
$Q_{\bar{A}}Q_{\bar{A}}$ total decay	~40%	–
(After 40 min)	~30%	~30% (~25%)[b]
Fast ($t_{1/2}$~100-200 s)	~15%	<20% (<17%)
Slow ($t_{1/2}$~40-60 min)	~25%	10–30% (9–25%)
Stable	~60%	–
(After 40 min)	~70%	~70% (60%)
Cytochrome b_{559}	30–50%	30–50%
Chlorophyll	<5%	?
Carotenoid	<1%	?
Split signal	–	~15%
g~2 radical		
Total	–	20–30%
$t_{1/2}$~40 min		10–15%
Stable		10–15%

[a] Complete turnover by cryogenic illumination is difficult in EPR samples due to inefficiencies in sample illumination within the EPR cavity and the highly dispersive nature of the kinetics of $Q_{\bar{A}}$ formation at 5 K [41]. Total quantification of all EPR donors generally does not exceed 85% of all centers as determined by Y_D. signal integration.
[b] Estimated $Q_{\bar{A}}$ decay (at a percentage of total centers). Calculated by multiplying the observed $Q_{\bar{A}}$ decay by 0.85.

The decay trace (Fig. 3A, solid red line) is biphasic over 40 min at 5 K and the components that are lost amount to ~30% of total $Q_{\bar{A}}$ generated. The measurement time was too short to resolve each $Q_{\bar{A}}$ decay component precisely and stability limitations of the instrument made longer measurements unreliable. However, an (upper bound) estimate of the magnitude of the fast component could be made from the loss of $Q_{\bar{A}}$ signal intensity after ~20 min dark adaptation (Fig. 3B, dashed red line) compared to that under saturating illumination (10 min, Fig. 3B solid line). The $Q_{\bar{A}}$ re-oxidation was found to be ~20% of the total $Q_{\bar{A}}$ generated.

To rule out changes in $Q_{\bar{A}}$ induction, decay or absorption behavior due to the presence of formate, control optical measurements were performed and compared to those presented above (Figs. 1 and 2). No significant changes were observed (data not shown).

Interestingly, it was found that once a sample has been exposed to saturating illumination, the fast re-oxidizing $Q_{\bar{A}}$ could be repeatedly re-reduced by the application of short illuminations (10 s) after allowing the sample to dark adapt for 10–20 min. In this way, the decay rate of the fast component could be extracted (Fig. 3C, open circles). It was observed that the decay of the $Q_{\bar{A}}$ signal was then mono-exponential, giving a $t_{1/2}$ of ~150 s. This could then be compared to the decay of the EPR split signal induced in the same sample, as measured at the low field peak (see below for details). Control experiments showed that the induction of the split signal was not affected by the presence of formate (Supporting information Fig. S7). The split signal decay kinetics is overlaid in Fig. 3C, and it is very similar to that of the $Q_{\bar{A}}Fe^{2+}$ signal. A single exponential fit of the split signal decay kinetics yields a $t_{1/2}$ of ~160 s. This correspondence in decay rates demonstrates a direct relationship between the decay of these two signals, and suggests that the radical responsible for the split signal is the same as that responsible for the fast component of the $Q_{\bar{A}}$ decay kinetics.

3.2.2. Resolution of different donors to $P680^+$ as observed by EPR spectroscopy

Complementary to the optical spectroscopy experiments described above, parallel EPR experiments were performed to observe EPR-visible radical species that were generated by low temperature illumination of PS II membranes. Overall, three signals were found.

Cytochrome b_{559} oxidation was evidenced by the well-characterized feature at g~3, corresponding to the g_x component of this radical (Fig. 4A). This signal was found to slowly accumulate with illumination time, with maximum signal intensity being reached after hour(s) long illumination. The cytochrome signal was stable once generated at

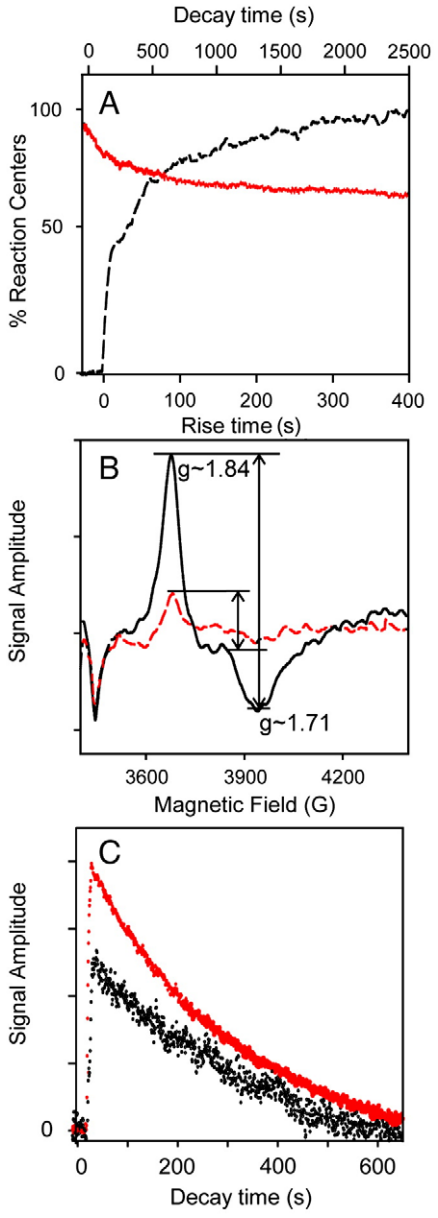

Fig. 3. Comparison of $_{Q_A-}$ and split signal decay kinetics as observed by EPR spectroscopy. (A) Time course of $Q_{\bar{A}}Fe^{2+}$, g~1.84 EPR signal intensity in PS II membranes (40% glycerol) treated with 25 mM sodium formate. Dashed black line: signal generation at 5 K as a function of the illumination time. Illumination starts time = 0. Solid red line: signal decay as a function of dark adaptation time at 5 K. $Q_{\bar{A}}Fe^{2+}$ signal monitored at field of signal maximum (g~1.84). Illumination ended at time = 0. (B) (Under illumination) minus (pre-illumination) difference spectrum (solid black line) and (under illumination) minus (20 min post illumination) difference spectrum (dashed red line) of the $Q_{\bar{A}}Fe^{2+}$ resonance (same sample as A). (C) Split signal decay kinetics (filled red circles) overlaid on fast $Q_{\bar{A}}Fe^{2+}$ decay kinetics (open circles; see text for details). Both observed in the dark immediately following 10 s illumination at 5 K (same sample as A; both signals measured in the presence of formate). The sample had experienced a saturating illumination and 10 min dark adaptation prior to the 10 s re-illumination (fast rise region). The $Q_{\bar{A}}Fe^{2+}$ decay curve is an average of three successive measurement cycles. The induced split signal was measured at the g~2.035 shoulder (see Fig. 4B). Total $Q_{\bar{A}}Fe^{2+}$ levels were estimated by a difference of the signal intensities at the g~1.84 and g~1.71 field positions, acquired in separate kinetic scans EPR parameters. (A and B): Microwave power 16 mW; frequency, 9.44 GHz; modulation amplitude, 32 G; time constant 2.6 s. (C): Microwave power, 6 mW (split), 16 mW (Q_A-); frequency 9.44 GHz, modulation amplitude, 10 G (split), 32 G (Q_A-); time constant, 0.5 s.

<20 K, and showed no decay upon subsequent dark adaptation. By comparing the increase in amplitude of this feature to that observed in a fully oxidized standard, an estimate was made of its donor contribution (with appropriate scaling via Y_D.). It was found that the amount of illumination-induced cytochrome b_{559} oxidation was typically 30–50%. This is consistent with the optical experiments above; where cytochrome b_{559} was also found to be stably induced by illumination in 30–50% of the PS II centers present (Table 1).

At the $g \sim 2$ region, two other signals with different decay kinetics could be observed. The faster decaying signal gave a $t_{1/2} \sim 100$–120 s, while the slower decaying signal was found to decay with $t_{1/2} \sim 40$–60 min, though a stable, non-decaying component of this signal was also observed.

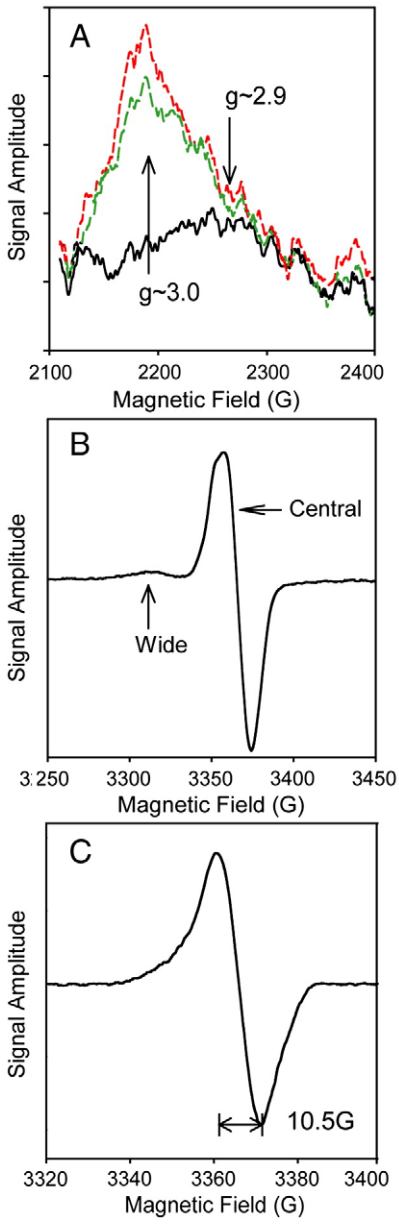

Fig. 4. EPR observed cryogenic donors to $P680^+$ produced by illumination at 5 K in 40% glycerol cryoprotectant. A: $g \sim 3$ (g_x) turning point of the oxidized cytochrome b_{559} (8.5 K). Solid black line:—pre-illumination; long green dashed line:—after 10 minutes illumination; short red dashed line:—after 1 h illumination. B: split signal observed under illumination at 5 K (both $Y_D^{\bullet}$ and 10.5 G radical subtracted). Labeled are the two main features associated with the signal when generated by visible illumination: a derivative centered at $g \sim 2.0$ and an absorption feature with maximum at $g \sim 2.035$. This appears to be the low field edge of a broad derivative like feature, the up-field negative component of which is partly overlaid by the prominent $g \sim 2$ peak. C: featureless, slowly decaying radical ($g \sim 2$, 10.5 G wide) generated upon illumination. EPR parameters: microwave power (A) 6 mW, (B) 50 μW, (C) 5 μW; frequency 9.44 GHz; modulation amplitude (A) 20 G, (B) 10 G, (C) 4 G.

In order to extract the spectral shape of the faster decaying signal, a difference spectrum was calculated from the signal taken under continuous illumination and that taken after the illuminated sample had been allowed to dark adapt for 10 min (Fig. 4B). This represents the component which decays within the first 10 min after illumination. This procedure minimized the contribution from the slowly decaying species whilst still allowing observation of the fast decaying signal with good signal-to-noise levels. The faster decaying signal was found to correspond to the S_1 state split signal, as previously reported [12,21], exhibiting both an assumed split derivative ($g \sim 2.035$, wide component) and a simple derivative feature centered at $g \sim 2.0$ (central component). The high field edge of the wide component appears only partially resolved as it overlays the more intense central component. Double integration of the total signal (scaled to Y_D.) yields an intensity of ~15% of centers.[2] It was further found that short illuminations (~1 min) were sufficient to generate the maximum signal, that the signal could also be re-generated at temperatures <20 K repeatedly without loss (its intensity was reproducible to within 10% over 5 successive illumination/decay cycles, with each cycle lasting more than 1 h in total).

Finally, in order to focus on the slowly decaying radical, a difference was taken between the spectrum of the sample before illumination and that of the sample after illumination and a subsequent ~15 min period of dark adaptation. This dark adaptation period allowed the fast decaying signal to decay away, so that the resulting difference spectrum consists only of the slowly decaying component of the total illumination-induced signal. This protocol also cancels out any contribution from the stable Y_D. radical. The resulting signal (Fig. 4C) is a featureless radical centered at $g \sim 2.0024$ with a width of 10.5 G. Its total donor contribution (scaled to Y_D) is typically 20–30%. As with cytochrome b_{559} oxidation, it slowly accumulated with illumination time, achieving maximum signal intensity after hour(s) long illumination.

Apart from their decay kinetics, the two signals found in the $g \sim 2$ region also differed from each other in their relaxation behavior, with the faster decaying split signal also being the faster relaxing of the two species (the signals shown in Fig. 4B and C were measured under their respective non-saturating conditions). This is explored further below.

3.2.3. Identifying distinct components of the split signal by $P_{1/2}$ studies

When examining the split signal (Fig. 4C) at a single applied microwave power, its spectral shape was found to be similar to those examples reported previously [12,21,30,31]. The spectral shape of the split signal was also independent of the presence or absence of exogenous electron acceptors (e.g. PpPQ). Only minor variations in the relative intensity of the wide and central components were observed between samples, probably reflecting changes in the relative microwave saturation properties of different components of the signal (see below). Contribution from the narrow, more stable radical signal is minimized through the subtraction protocol described above. As previously reported [12,30], neither component of the split signal was generated in material lacking the manganese cluster (e.g. via Tris or NH_2OH treatments; data not shown), whereas a central component remained in the presence of methanol [32]. The use of 40% glycerol (v/v) as a cryoprotectant did not affect split signal yields.

[2] Assuming the broad split signal arises from a weak interaction between a spin 1/2 radical and some higher spin center of which the effective Zeeman energy (reflected by the g value) differs from that of the radical by substantially more than their interaction energy, then this estimation is valid. That is, the radical's absorption is simply spread over a wider field range, but the total transition intensity is unaltered in first order.

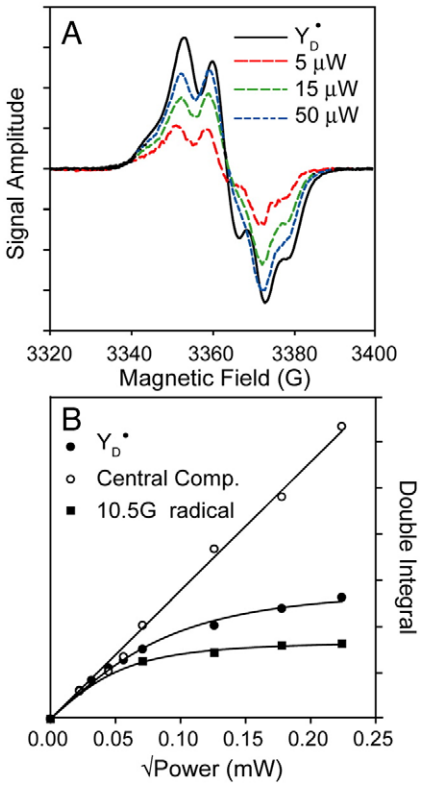

Fig. 5. Characterization of the central component of the split signal. (A) The central component of the split signal (Fig. 3B, $g \sim 2.0$) observed at low modulation amplitude and various microwave powers. Superimposed is the scaled Y_D. spectrum (solid line). (B) The signal intensity as a function of the square root of the microwave power at 5 K of (i) 10.5 G radical (filled squares), (ii) Y_D. (filled circles), and (iii) central split signal component (open circles). Sample conditions and EPR parameters as in Fig. 4C except: modulation amplitude, 4 G; sweep width is 100 G.

It was observed that, at low microwave powers and modulation amplitudes, the central component of the split signal could be resolved to give a hyperfine structure indicative of an oxidized tyrosine (Fig. 5A). This was the case even where methanol was present in the sample (4%; data not shown). This is in agreement with literature proposals that Y_Z. is the radical species that interacts with the $CaMn_4$ cluster to give the split signals, and recent similar observations of such a tyrosine-shaped component in split signal when measured at high temperatures (~100 K) [33,34].

In addition, the central component was found to be a faster relaxing species when compared to the slower relaxing Y_D., or the even more slowly relaxing 10.5 G radical. The signal was unsaturated at 50 μW. By contrast, Y_D. was found to give a $P_{1/2}$ of ~10 μW, consistent with literature values [35]. The $P_{1/2}$ of the 10.5 G radical was lower still, at 5 μW, suggesting that it may arise from an organic radical well removed from any fast-relaxing paramagnetic center in PS II. Thus the faster relaxation rate of the central component of the split signal is again evidence that it represents Y_Z., situated in close proximity to the $CaMn_4$ cluster.

Finally, as compared to Y_D., the central component of the split signal may have an altered hyperfine pattern and a possible shift in apparent g value. Since this difference was seen at all powers up to 50 μW, it is unlikely to result from contamination by other radical species.

Significantly, it was found that the spectral shape of this tyrosine-like central component was essentially constant over the microwave power range used (Fig. 5A), suggesting that the pattern is homogeneous with no interference from an underlying, slowly relaxing component (i.e. Y_D). The spectral shape was also preserved across a range of temperatures (5 K–20 K, Supporting information S4). This provides confirmation that the subtraction procedure for obtaining the split signal was successful in minimizing contributions from both the stable 10.5 G radical, and that the resolved tyrosine structure is not simply a saturation artifact of the large Y_D background due to enhancement of Y_D. relaxation rate upon split signal induction (i.e. the influence of another paramagnetic center in the vicinity of Y_D).

4. Discussion

4.1. Quantitative analysis of turnover

4.1.1. Carotenoid/chlorophyll oxidation

Our optical measurements essentially exclude chlorophyll or carotenoid pigment oxidation following cryogenic turnover in the S_1 state of PS II in plant membranes, as prepared here [26]. Significant donation from either of these species does not occur upon low temperature illumination in this PS II preparation, either transiently or statically, irrespective of split signal intensity. However, as we will discuss elsewhere (see author's note), this result is dependant on the details of the PS II membrane preparation procedure used and is probably influenced to some extent by the illumination regime employed. The results seen here appear to represent one limit of a spectrum of behaviors that plant PS II preparations can exhibit.

The lack of carotenoid oxidation seen here contrasts with earlier studies where the pigment has been shown to be the dominant electron donor in higher plant PS II at liquid He temperatures. In these circumstances the cytochrome b_{559} center was pre-oxidized [6]. We find that a significant yield of photo-induced carotenoid oxidation occurs in PS II membrane samples subject to further detergent treatment during preparation, such that cytochrome b_{559} is almost totally oxidized before cryogenic illumination. Nevertheless, we are unable to achieve more than ~50% of cryogenic donor contribution from carotenoid even in these samples. Previous optical studies may have over-estimated carotenoid involvement [4,6]. In these investigations there was no direct measure of charge transfer (i.e. $Q_{\bar{A}}$ formation) and so carotenoid turnover was scaled to total absorbance rather than an internal reaction center count.

Previous work has also correlated either carotenoid and chlorophyll cation radical formation with the appearance of featureless EPR signal(s) at $g \sim 2$, of width 9.5–10.5 G [4,6,21]. Such an assignment may now require qualification, at least for minimally detergent-treated PS II samples as used here, since we observe a similar featureless photogenerated derivative EPR signal (~30% of Y_D.) in the absence of any chlorophyll or carotenoid oxidation. A non-pigment, non-tyrosine ('mystery', see below) donor may thus be present, which would be difficult to distinguish from Chl^+ or Car^+ radicals in conventional low field EPR.

4.1.2. Cytochrome/$Q_{\bar{A}}$ balance

The only donor oxidation that could be observed in optical spectroscopy was that of cytochrome b_{559}. By scaling to a dithionite-treated standard, where all cytochrome b_{559} is in its reduced form, the extent of cytochrome oxidation relative to reaction centers that undergo charge separation (as measured by $Q_{\bar{A}}$ formation) could be quantified. It was clear that cytochrome oxidation could not account for all illumination-induced $Q_{\bar{A}}$ formation. Similar quantification results were obtained via EPR spectroscopy. Furthermore, while $Q_{\bar{A}}$ was found to partially re-oxidize upon dark adaptation at 5 K, presumably via charge recombination pathways, oxidized cytochrome remained stably oxidized at 5 K. Subsequent sample re-illuminations generated no more oxidized cytochrome species. Therefore, while cytochrome oxidation is likely to be account for a substantial portion of PS II centers with stably reduced $Q_{\bar{A}}$ after illumination (Table 1), the decaying components of $Q_{\bar{A}}$ could not be accounted for by any donor species with a readily accessible optical signature.

4.1.3. $Q_{\bar{A}}$ decay-split signal involvement

Zhang et al. [36] demonstrated the S_1 split EPR signal of thermophilic cyanobacteria decayed together with the $Q_{\bar{A}}Fe^{2+}$ resonance at $g\sim1.9$. As this signal is small and appears close to intense signals in the $g\sim2$ region, they also measured the $Q_{\bar{A}}/Fe^{2+}/Q_{\bar{B}}$ signal at $g\sim1.6$ [37], showing a similar effect. From this result they concluded that the split signal species was most likely a donor to $P680^+$, relaxing at 5 K via charge recombination.

Our experiments here on the signal using spinach PS II membranes confirm the observations of Zhang et al. [36]. $Q_{\bar{A}}$ decayed with the same half-life as the split signal resonance in approximately ~20% of centers that had undergone charge separation. This was consistent with our optical quantification (Fig. 2 and Table 1). We additionally found that the use of formate treatment [29] to enhance the $Q_{\bar{A}}/Fe^{2+}$ signal led to no changes in split signal formation. Apart from allowing more reliable quantification due to the enhanced intensity of the $Q_{\bar{A}}/Fe^{2+}$ signal, this observation is good evidence that the acceptor side of PS II, namely $Q_{\bar{A}}$ is not involved in the split signal. This can be compared to literature reports where formate alters the $Pheo_{\bar{D}1}/Q_{\bar{A}}$ spin–spin interaction, changing the splitting and signal width of the $Pheo_{\bar{D}1}$ split signal [29].

4.1.4. New redox center (stable 'mystery donor')

An interesting finding from a correlation of our parallel optical and EPR measurements is that the featureless 10.5 G wide radical as seen by EPR has no obvious optical signature in the visible/near IR region. This radical was found to decay slowly during dark adaptation after its induction by cryogenic illumination, allowing it to be isolated from the faster decaying split signal. It was also found to undergo slow paramagnetic relaxation compared to (both components of) the split signal, and its $P_{1/2}$ value was comparable to that of Y_D.. These factors suggest that it is a magnetically isolated radical species in the protein matrix, possibly derived from an amino acid residue. The width of the EPR resonance suggests that it is a large molecule, and its g value (~2.002) and absence of characteristic proton hyperfine splitting features argue against an assignment to tyrosine. Another possible candidate is a tryptophan side chain, which should be detectable in the UV (<300 nm) region.

4.1.5. EPR of S_1 split signal; a 'tyrosine-like' component

The match between the fast phase of the Q_A^- decay kinetics and the split signal decay kinetics, together with the fact that a fast-relaxing, transient tyrosine radical was found by EPR spectroscopy in the $g\sim2$ region upon induction of the split signal, strongly suggest Y_Z. involvement in the split signal. This is consistent with previous literature proposals, but is the first demonstration of the fact at those cryogenic temperatures (<10 K) at which the split species is directly observed.

The transient tyrosine signal may correspond to the '26 G fast decaying' signal first seen by [20]. This signal did not resolve a hyperfine coupling, but has approximately the same width and decay kinetics as the transient tyrosine signal observed here. It was reported that the '26 G' signal was not observed in samples containing 40% glycerol. As the addition of glycerol did not have any effect on S_1 split signal (shape or yield) for our PS II preparation, we suspect our samples resemble 'untreated PS II' as defined in [20] and therefore could potentially resolve a '26 G fast decaying' signal. However, we cannot exclude the possibility that this signal is separate from the '26 G signal', akin to the light-induced tyrosine signal observed in methanol containing samples.

Acknowledgements

The authors are grateful to Mr. K. Jackson for invaluable technical assistance. F. Ho acknowledges the financial support of the European Union Sixth Framework Programme Marie Curie Incoming International Fellowship (514817). S Styring acknowledges support from the Swedish Research Council and the Swedish Energy Agency. E. Krausz and R Pace acknowledge support from the Australian Research Council.

Appendix A. Supplementary data

Supplementary data associated with this article can be found, in the online version, at doi:10.1016/j.bbabio.2009.03.023.

References

[1] K. Ahrling, R.J. Pace, M.C.W. Evans, The Catalytic Manganese Cluster: Implications from Spectroscopy, Vol. 1, Springer, 2005.
[2] J.C. de Paula, J.B. Innes, G.W. Brudvig, Electron transfer in photosystem II at cryogenic temperatures, Biochemistry 24 (1985) 8114–8120.
[3] L.K. Thompson, G.W. Brudvig, Cytochrome *b*-559 may function to protect photosystem II from photoinhibition, Biochemistry 27 (1988) 6653–6658.
[4] P. Faller, A. Pascal, A.W. Rutherford, b-Carotene redox reactions in photosystem II: electron transfer pathway, Biochemistry 40 (2001) 6431–6440.
[5] J.S. Vrettos, D.H. Stewart, J.C. de Paula, G.W. Brudvig, Low-temperature optical and resonance raman spectra of a carotenoid cation radical in photosystem II, J. Phys. Chem. B 103 (1999) 6403–6406.
[6] J. Hanley, Y. Deligiannakis, A. Pascal, P. Faller, A.W. Rutherford, Carotenoid oxidation in photosystem II, Biochemistry 38 (1999) 8189–8195.
[7] C.A. Tracewell, G.W. Brudvig, Two redox-active b-carotene molecules in photosystem II, Biochemistry 42 (2003) 9127–9136.
[8] C.A. Tracewell, A. Cua, D.H. Stewart, D.F. Bocian, G.W. Brudvig, Characterization of carotenoid and chlorophyll photooxidation in photosystem II, Biochemistry 40 (2001) 193–203.
[9] C.A. Buser, L.K. Thompson, B.A. Diner, G. Brudvig, Electron-transfer reactions in manganese-depleted photosystem II, Biochemistry 29 (1990) 8977–8985.
[10] A. Cua, D.H. Stewart, G.W. Brudvig, D.F. Bocian, Selective resonance raman scattering from chlorophyll Z in photosystem II via excitation into the near-infrared absorption band of the cation, J. Am. Chem. Soc. 120 (1998) 4532–4533.
[11] K.V. Lakshmi, O.G. Poluektov, M.J. Reifler, A.M. Wagner, M.C. Thurnauer, G.W. Brudvig, Pulsed high-frequency EPR study on the location of carotenoid and chlorophyll cation radicals in photosystem II, J. Am. Chem. Soc. 125 (2003) 5005–5014.
[12] J.H.A. Nugent, P. Muhiuddin, M.C.W. Evans, Electron transfer from the water oxidizing complex at cryogenic temperatures: the S1 to S2 step, Biochemistry 41 (2002) 4117–4126.
[13] A. Boussac, J.-L. Zimmermann, A.W. Rutherford, EPR signals from modified charge accumulation states of the oxygen-evolving enzyme in Ca2+-deficient photosystem II, Biochemistry 28 (1989) 8984–8989.
[14] M. Sivaraja, J. Tso, G.C. Dismukes, A calcium specific site influences the structure of and activity of the manganese cluster responsible for photosynthetic water oxidation, Biochemistry 28 (1989) 9459–9464.
[15] D.J. Maclachlan, J.H.A. Nugent, Investigation of S3 electron paramagnetic resonance signals from the oxygen-evolving complex of photosystem 2: effect of inhibition of oxygen evolution by acetate, Biochemistry 32 (1993) 9772–9780.
[16] P. Dorlet, M.D. Valentin, G.T. Babcock, J.L. McCracken, Interaction of YZ with its environment in acetate-treated photosystem II membranes and reaction center cores, J. Phys. Chem. B 102 (1998) 8239–8247.
[17] K.V. Lakshmi, S.S. Eaton, G.R. Eaton, H.A. Frank, G.W. Brudvig, Analysis of dipolar and exchange interactions between manganese and tyrosine Z in the S2YZ; state of acetate-inhibited photosystem II via EPR spectral simulations at X- and Q-bands, J. Phys. Chem. B 102 (1998) 8327–8335.
[18] J.M. Peloquin, K.A. Campbell, R.D. Britt, 55 Mn pulsed ENDOR demonstrates that the photosystem II "split" EPR signal arises from a magnetically-coupled magnano-tyrosyl complex, J. Am. Chem. Soc. 120 (1998) 6840–6841.
[19] D. Koulougliotis, J.-R. Shen, N. Ioannidis, V. Petrouleas, Near-IR irradiation of the S2 state of the water oxidizing complex of photosystem II at liquid helium temperatures produces the metalloradical intermediate attributed to S1YZ, Biochemistry 42 (2003) 3045–3053.
[20] G. Sioros, D. Koulougliotis, G. Karapanagos, V. Petrouleas, The S1YZ; metalloradical EPR signal of photosystem II contains two distinct components that advance respectively to the multiline and $g=4.1$ conformations of S2, Biochemistry 46 (2007) 210–217.
[21] K.G.V. Havelius, J.-H. Su, Y. Feyziyev, F. Mamedov, S. Styring, Spectral resolution of the split EPR signals induced by illumination at 5 K from the S1, S3, and S0 states in photosystem II, Biochemistry 45 (2006) 9279–9290.
[22] J.H. Su, K.G.V. Havelius, F.M. Ho, G. Han, F. Mamedov, S. Styring, Formation spectra of the EPR split signals from the S0, S1, and S3 states in photosystem II induced by monochromatic light at 5 K, Biochemistry 46 (2007) 10703–10712.
[23] N. Ioannidis, G. Zahariou, V. Petrouleas, Trapping of the S2 to S3 state intermediate of the oxygen-evolving complex of photosystem II, Biochemistry 45 (2006) 6252–6259.
[24] T.M. Bricker, H.B. Pakrasi, L.A. Sherman, Characterization of a spinach photosystem II core preparation isolated by a simplified method, Arch. Biochem. Biophys. 237 (1985) 170–176.

[25] P.J. Smith, K.A. Ahrling, R.J. Pace, Nature of the S2 state electron paramagnetic resonance signals from the oxygen-evolving complex of photosystem II: Q-band and oriented X-band studies, J. Chem. Soc., Faraday Trans. 89 (1993) 2863–2868.
[26] P.J. Smith, S. Peterson, M. Masters, T. Wydrzynski, S. Styring, E. Krausz, R.J. Pace, Magneto-optical measurements of the pigments in fully active photosystem II core complexes from plants, Biochemistry 41 (2002) 1981–1989.
[27] J.L. Hughes, P. Smith, R. Pace, E. Krausz, Charge separation in photosystem II core complexes induced by 690–730 nm excitation at 1.7 K, Biochim. Biophys. Acta - Bioenergetics 1757 (2006) 841–851.
[28] S. Peterson, M. Masters, B.J. Prince, P.J. Smith, R.J. Pace, E. Krausz, Optical spectra of synechocystis and spinach photosystem II preparations at 1.7 K: identification of the D1-pheophytin energies and stark shifts, J. Am. Chem. Soc. 125 (2003) 13063–13074.
[29] A.W. Rutherford, J.L. Zimmermann, A new EPR signal attributed to the primary plastosemiquinone acceptor in photosystem II, Biochim. Biophys. Acta - Bioenergetics 767 (1984) 168–175.
[30] C. Zhang, S. Styring, Formation of split electron paramagnetic resonance signals in photosystem II suggests that tyrosine Z can be photooxidized at 5 K in the S0 and S1 states of the oxygen-evolving complex, Biochemistry 42 (2003) 8066–8076.
[31] D. Koulougliotis, C. Teutloff, Y. Sanakis, W. Lubitz, V. Petrouleas, The S1YZ. Metalloradical intermediate in photosystem II: an X- and W-band EPR study, Phys. Chem. Chem. Phys. 6 (2004) 4859–4863.
[32] J.-H. Su, K.G.V. Havelius, F. Mamedov, F.M. Ho, S. Styring, Split EPR signals from photosystem II are modified by methanol, reflecting S state-dependent binding and alterations in the magnetic coupling in the CaMn4 cluster, Biochemistry 45 (2006) 7617–7627.
[33] N. Ioannidis, G. Zahariou, V. Petrouleas, The EPR spectrum of tyrosine Z; and its decay kinetics in O2-evolving photosystem II preparations, Biochemistry 47 (2008) 6292–6300.
[34] G. Zahariou, N. Ioannidis, G. Sioros, V. Petrouleas, The collapse of the tyrosine Z-Mn spin–spin interaction above ~100 K reveals the spectrum of tyrosine Z. An application of rapid-scan EPR to the study of intermediates of the water splitting mechanism of photosystem II, Biochemistry 46 (2007) 14335–14341.
[35] R.G. Evelo, S. Styring, A.W. Rutherford, A.J. Hoff, EPR relaxation measurements of photosystem II reaction centers: influence of S-state oxidation and temperature, Biochim. Biophys. Acta 973 (1989) 428–442.
[36] C. Zhang, A. Boussac, A.W. Rutherford, Low-temperature electron transfer in photosystem II: a tyrosyl radical and semiquinone charge pair, Biochemistry 43 (2004) 13787–13795.
[37] B. Hallahan, S. Ruffle, S. Bowden, J.H.A. Nugent, Identification and characterisation of EPR signals involving QB semiquinone in plant Photosystem II, Biochim. Biophys. Acta 1059 (1991) 181–188.